

455  
11/10/80 TS

DOE/JPL/955640-80/2

12. 1988

## DEVELOPMENT AND FABRICATION OF A SOLAR CELL JUNCTION PROCESSING SYSTEM

MASTER

Quarterly Progress Report No. 2

July 1980

Work Performed Under Contract No. NAS-7-100-955640

Spire Corporation  
Bedford, Massachusetts



# U.S. Department of Energy



**Solar Energy**

DISTRIBUTION OF THIS DOCUMENT IS UNLIMITED

## **DISCLAIMER**

**This report was prepared as an account of work sponsored by an agency of the United States Government. Neither the United States Government nor any agency Thereof, nor any of their employees, makes any warranty, express or implied, or assumes any legal liability or responsibility for the accuracy, completeness, or usefulness of any information, apparatus, product, or process disclosed, or represents that its use would not infringe privately owned rights. Reference herein to any specific commercial product, process, or service by trade name, trademark, manufacturer, or otherwise does not necessarily constitute or imply its endorsement, recommendation, or favoring by the United States Government or any agency thereof. The views and opinions of authors expressed herein do not necessarily state or reflect those of the United States Government or any agency thereof.**

## **DISCLAIMER**

**Portions of this document may be illegible in electronic image products. Images are produced from the best available original document.**

## DISCLAIMER

"This book was prepared as an account of work sponsored by an agency of the United States Government. Neither the United States Government nor any agency thereof, nor any of their employees, makes any warranty, express or implied, or assumes any legal liability or responsibility for the accuracy, completeness, or usefulness of any information, apparatus, product, or process disclosed, or represents that its use would not infringe privately owned rights. Reference herein to any specific commercial product, process, or service by trade name, trademark, manufacturer, or otherwise, does not necessarily constitute or imply its endorsement, recommendation, or favoring by the United States Government or any agency thereof. The views and opinions of authors expressed herein do not necessarily state or reflect those of the United States Government or any agency thereof."

This report has been reproduced directly from the best available copy.

Available from the National Technical Information Service, U. S. Department of Commerce, Springfield, Virginia 22161.

Price: Paper Copy \$6.00  
Microfiche \$3.50

DRD No. QR  
CDRL Item No. 5

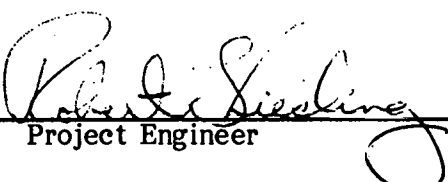
DEVELOPMENT AND FABRICATION OF A  
SOLAR CELL JUNCTION PROCESSING SYSTEM

Report Number QR-10073-02  
Quarterly Report

July 1980

This work was performed for the Jet Propulsion  
Laboratory, California Institute of Technology  
sponsored by the National Aeronautics and Space  
Administration under Contract NAS7-100.

Prepared by:



Robert Sieckling

Project Engineer

Approved by:



J. L. Cerni

Program Manager

SPIRE CORPORATION

Patriots Park

Bedford, MA 01730



THIS PAGE  
WAS INTENTIONALLY  
LEFT BLANK

## TABLE OF CONTENTS

<u>Section</u>		<u>Page</u>
1	CONTRACT OBJECTIVES . . . . .	1
2	SUMMARY OF WORK PERFORMED. . . . .	3
	2.1 Introduction . . . . .	3
	2.2 Developmental Testing . . . . .	3
	2.3 Pulser Design . . . . .	3
3	PROGRESS ON TASK 1 - DEVELOPMENT OF PULSED ELECTRON BEAM SUBSYSTEM. . . . .	5
	3.1 Developmental Testing . . . . .	5
	3.1.1 Diode Experiments with Argon Gas . . . . .	5
	3.1.2 Wafer Preheat Experiments . . . . .	7
	3.1.3 Flame-Sprayed Metal Coatings . . . . .	7
	3.2 Pulser Design . . . . .	8
	3.2.1 Collimating Magnet Design . . . . .	10
	3.2.2 Power Supply and Charging Network for PEBA Energy Store . . . . .	12
	3.2.2.1 Resistive Charging . . . . .	13
	3.2.2.2 RC Charging System for 160 kV . . . . .	14
	3.2.2.3 Intermediate Storage Charging . . . . .	16
	3.2.2.4 Intermediate Storage Element Charging System for 300kV . . . . .	20
	3.2.2.5 RC Charging System for 300kV . . . . .	21
	3.2.3 Pressure Vessel and Energy Store Support Structure . . . . .	23
	3.2.4 Interim Wafer-Handling System . . . . .	24
	3.2.5 Electronic Control . . . . .	24
	3.2.6 Vacuum System . . . . .	24
4	PLANS . . . . .	28
5	SCHEDULE . . . . .	29

## LIST OF FIGURES

<u>Figure</u>		<u>Page</u>
1	Spire/JPL Junction Processor	2
2	Beam Parameters Versus Gas Pressure	6
3	SPI-PULSE 7000 Schematic Diagram	9
4	Resistive Charging Schematic	13
5	Series Resistor Incorporated into Multi-Element Dielectric Line Energy Store	17
6	Diagram of Intermediate Storage Element Charging System	18
7	SPI-PULSE 7000 Functional Block Diagram	25
8	SPI-PULSE 7000 System Schematic	26
9	Task 1 Schedule	30

## SECTION 1

### CONTRACT OBJECTIVES

The basic objectives of the program are the following:

1. To design, develop, construct and deliver a junction processing system which will be capable of producing solar cell junctions by means of ion implantation followed by pulsed electron beam annealing.
2. To include in the system a wafer transport mechanism capable of transferring 4-inch-diameter wafers into and out of the vacuum chamber where the ion implantation and pulsed electron beam annealing processes take place.
3. To integrate, test and demonstrate the system prior to its delivery to JPL along with detailed operating and maintenance manuals.
4. To estimate component lifetimes and costs, as necessary for the contract, for the performance of comprehensive analyses in accordance with the Solar Array Manufacturing Industry Costing Standards (SAMICS).

In achieving these objectives, Spire will perform five tasks:

Task 1 - Pulsed Electron Beam Subsystem Development

Task 2 - Wafer Transport System Development

Task 3 - Ion Implanter Development

Task 4 - Junction Processing System Integration

Task 5 - Junction Processing System Cost Analyses

Under this contract the automated junction formation equipment to be developed involves a new system design incorporating a modified, government-owned, JPL-controlled ion implanter into a Spire-developed pulsed electron beam annealer and wafer transport system. Figure 1 presents a conceptual drawing of the junction processing system. When modified, the ion implanter will deliver a 16 mA beam of  $^{31}\text{P}^+$  ions with a fluence of  $2.5 \times 10^{15}$  ions per square centimeter at an energy of 10 keV. The throughput design goal rate for the junction processor is  $10^7$  four-inch-diameter wafers per year.

At the present time, authorization has been given to perform work only on Task 1. The performance of Tasks 2, 3, 4 and 5 has been deferred until a written "Notice to Proceed" with one more of these deferred tasks is received from JPL.

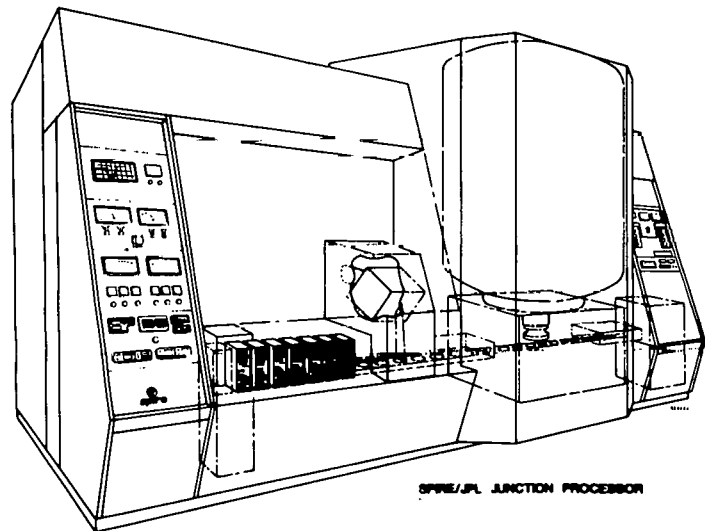


FIGURE 1. SPIRE/JPL JUNCTION PROCESSOR

## SECTION 2

### SUMMARY OF WORK PERFORMED

#### 2.1 INTRODUCTION

This 2nd Quarterly Report covers the period April 1 through June 30, 1980 for Task I of a contract for the development and fabrication of a solar cell junction processing system. Technical discussion in this report reviews the engineering design and support experiments underway for the prototype development of a pulsed electron beam annealing machine subsystem.

#### 2.2 DEVELOPMENTAL TESTING

Beam control experiments using argon gas in the diode were carried out to test the concept of using partial space charge and current neutralization to improve beam uniformity. At pressures up to 14 microns the beam could be used with a 2 mm anode-to-cathode diode gap. Doubling the gap to 4 mm allowed an increase in usable pressure to 25 microns with a tighter beam pinch at this higher pressure. The experiments did not show the anticipated advantages. However, acceptable annealing characteristics were seen at 25 microns with large gaps at lower charging voltages — implying that this arrangement might be one way to couple the energy store into the diode efficiently, keeping the average electron energy lower.

Using an infrared heater, wafers were preheated to 400°C in vacuum prior to electron beam pulse annealing to examine the influence of such heating on the annealing process. From the data obtained it was concluded that in the complete processing sequence, the finished cell characteristics would be identical for starting wafers pulsed cold or preheated when followed by any moderate heat treatment.

From an evaluation of a technique for metallization using a flame-spraying process, it appears that this method can be used in the fabrication of the dielectric storage line and for the application of a corrosion-resistant coating onto the interior of the steel pressure vessel.

#### 2.3 PULSER DESIGN

The mechanical design phase of the major elements of the electron beam pulser, designated SPI-PULSE 7000, has been completed with the drawings released to Manufacturing for fabrication.

The main frame structural support layout has been completed with vendor quotes being solicited for fabrication and delivery of the necessary construction hardware.

Electronic system control requirements continue to be identified along with the design and selection of the necessary components for the overall machine control, monitoring and safety circuits.

SECTION 3  
PROGRESS ON TASK 1 — DEVELOPMENT OF  
PULSED ELECTRON BEAM SUBSYSTEM

3.1 DEVELOPMENTAL TESTING

Until the completion of the pulsed electron beam subsystem, a smaller existing electron beam pulser, the SPI-PULSE 5000, is being used at Spire for the advanced design verification experiments.

3.1.1 Diode Experiments with Argon Gas

With pulsed beam currents approaching 50 kA, the conduction of this current away from the wafers during the annealing step is an important design consideration. If the electron beam could propagate in a low-density plasma, partial space charge and current neutralization of the beam would be provided by the low-energy ions and electrons in the plasma. Thus a lower net current would be carried to the surface of the wafer.

A series of experiments was performed on the SPI-PULSE 5000 in which argon gas was introduced into the diode region of the pulser. Modifications to the standard carousel vacuum-process chamber met the experimental requirement of maintaining a controlled and measured gas pressure in the diode region.

The argon was leaked into the back of the chamber through an ultrafine needle valve. The diffusion pumps were throttled down to maintain steady pressure values from 0.1 to 40 microns. The pressure was measured using a McLeod gauge for the higher pressure values and a calibrated thermocouple gauge for values below 10 microns.

Before conducting experiments the effect of the gas pressure on the beam was measured. Diode voltage and current monitor traces were used to determine the peak voltage, current and voltage pulse width, as shown in Figure 2. A standard carbon calorimeter was used to measure the fluence on the beam axis, and ion-implanted test wafers were used as witness plates to determine the beam profile. At a "maximum" pressure the charging voltage and magnetic field were varied to obtain a uniform anneal for constant fluence experiments.

Experiments were first performed using a standard 2-inch-beam setup with a 90 mil anode-to-cathode gap and a sample spacing of 5 mm. Calorimetry data was taken for pressures from 0.5 micron to 14 microns at a 150 kV charging voltage and a magnet

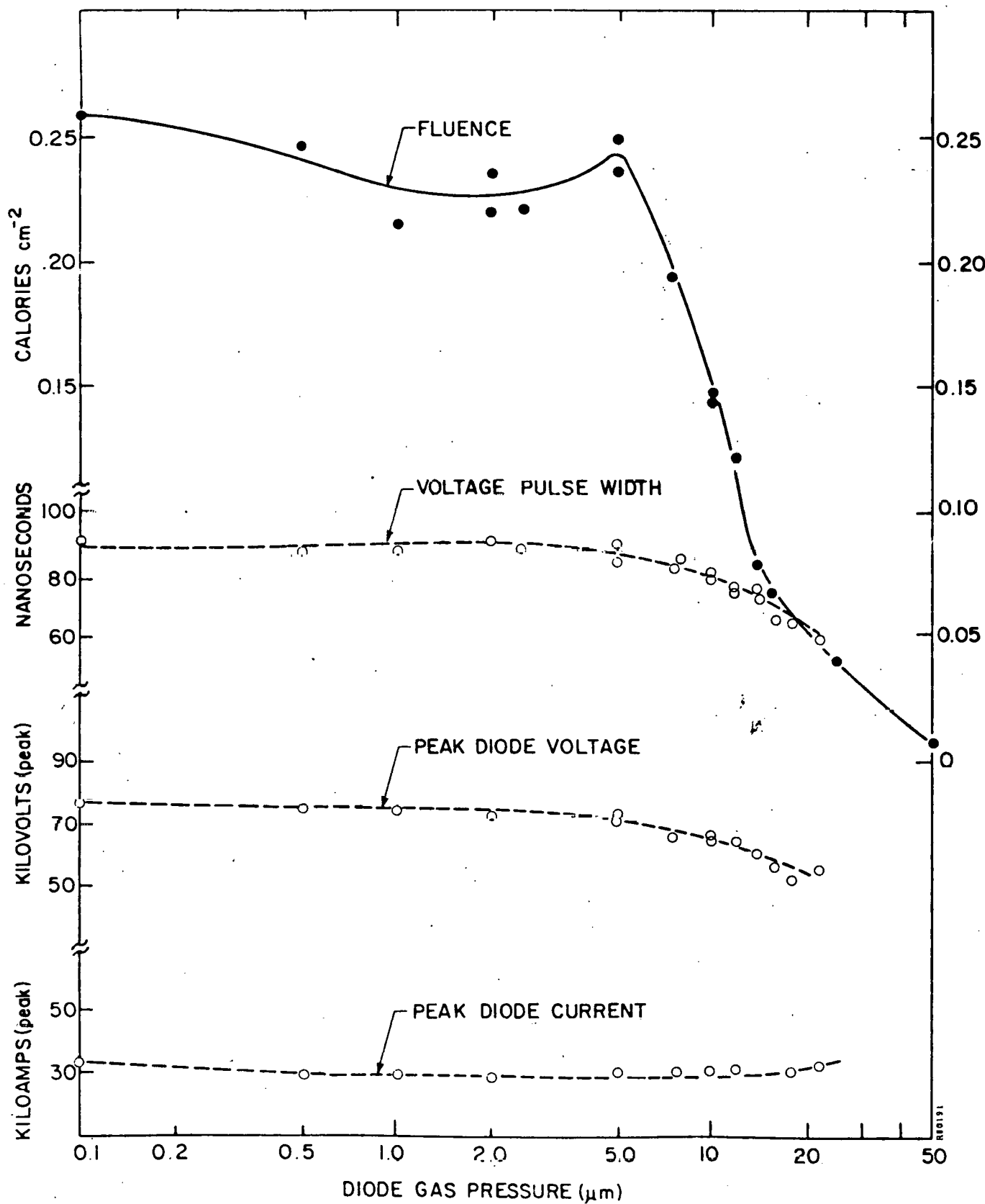


FIGURE 2. BEAM PARAMETERS VERSUS GAS PRESSURE

current of 3.2 A. The uppermost curve in Figure 2 presents the results of this data. Test wafers were shot at high vacuum, then at argon pressures from 6 to 22 microns. The high-vacuum anneal showed some weak spots. At 6 microns a weak center surrounded by an annular annealed region appeared and grew until fluence was almost totally lost at 22 microns. The outline of the anneal became more circular at 8 microns and remained so for higher pressures. These experiments showed that with an argon background gas, process chamber pressures higher than 14 microns would result in loss of useful beam fluence. Even though these experiments did not show a significant improvement in beam uniformity with increased diode gas pressure, another variable for beam control was identified to match the pulse generator load for large diode gaps.

### 3.1.2 Wafer Preheat Experiments

During ion implantation in a large-volume production line, the wafers will be heated to temperatures close to 100°C by the ion beam. Since this heating could influence the pulse annealing process, a number of experiments using a specially designed infrared wafer heater were initiated during this reporting period. The existing SPI-PULSE 5000 accelerator was used to carry out these tests. The infrared substrate heater allowed the test wafers to be heated in vacuum to temperatures through 400°C with only a 1°C per second temperature drop after heater turnoff. Early test results indicated that preheating followed by a cooldown period before pulsed electron beam annealing does not offer any advantage. However, wafers directly annealed by a pulsed electron beam while hot showed a more uniform anneal. Finished cell characteristics are identical for pulsing wafers cold or heated, if followed by a 400°C contact sinter. Further preheat testing is necessary to determine whether there could be any preheat advantage in elevating the damage threshold level.

### 3.1.3 Flame-Sprayed Metal Coatings

In the fabrication of the energy storage capacitors a conductive coating is used to form the outer conductor. In the past this outer conductor was formed using several layers of silver paint. As a less expensive means of forming this outer conductor, due to the large number of capacitor liners (19) required, an evaluation of a metallizing technique using a flame-spraying process was initiated. In this process, metal in wire form is drawn through a special gun by a pair of powered feed rolls. At the nozzle of the

gun the wire is continuously melted in an oxygen-fuel-gas flame and atomized by a compressed air blast which carries the metal particles to the previously prepared surface. The individual particles mesh to produce a coating of the desired metal. Results can be readily duplicated, since the supply and pressure of the oxygen-fuel-gas mixture and air are accurately controlled by flowmeters and pressure regulators.

The following metals were tried: aluminum, copper, nickel and zinc. Zinc, with its lower melting temperature ( $419^{\circ}\text{C}$ ), adhered well to the epoxy dielectric surface with a smoother interface finish as compared with the aluminum coatings. The flame-sprayed copper and nickel were found to be incompatible with the epoxy. It appears that the process is feasible for the liner fabrication, but final confirmation awaits high-voltage stress testing.

As a result of these evaluations this flame-spray technique has been selected to coat the interior walls of the steel pressure vessel and 5-foot-diameter dielectric support plate with a 3-7 mil thick aluminum coating to insure corrosion resistance and establish a good electrical ground path.

### 3.2 PULSER DESIGN

The configuration of the major system elements for the SPI-PULSE 7000 pulsed electron beam subsystem is illustrated in the schematic diagram of Figure 3. The final mechanical detail drawing packages have been released to Manufacturing for fabrication of the energy storage lines, overall energy storage tank, vacuum process chamber and internal support hardware.

The console electronics for the overall machine control and system monitoring are currently being designed with the data acquisition circuits breadboarded. The long lead-time electronic components have been identified and the purchase orders issued for their procurement.

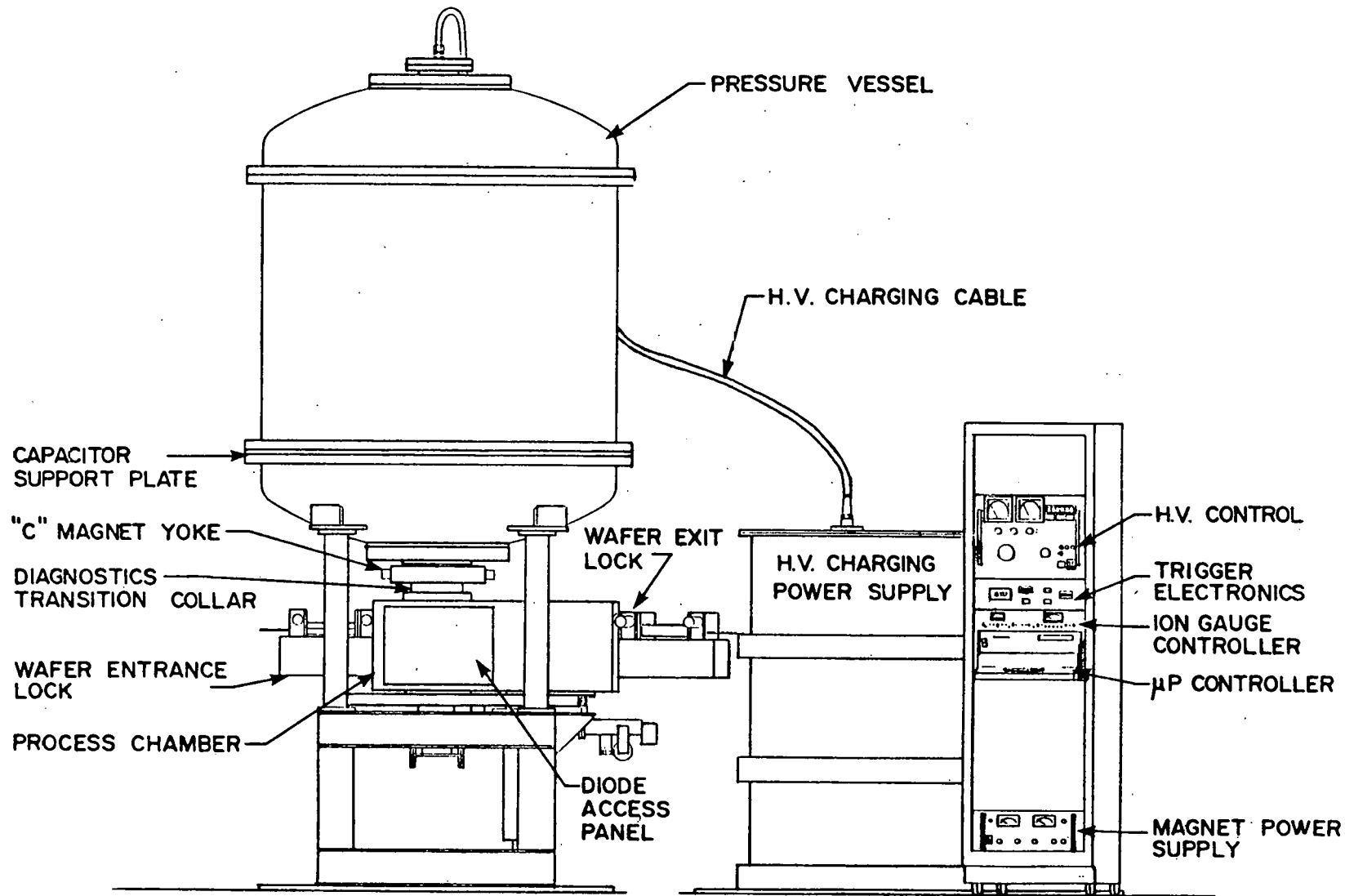


FIGURE 3. SPI-PULSE 7000 SCHEMATIC DIAGRAM

### 3.2.1 Collimating Magnet Design

The requirements for the electron beam collimating magnet to be used with the 7000 Pulse Annealer are listed below:

1. The magnetic field must be adjustable with a maximum flux density of 5000 gauss.
2. The magnetic field must be established in a region that is 6 inches in diameter and 2 inches long.
3. The magnetic field, in one configuration, must be relatively uniform throughout a 4-inch diameter region.
4. There should be a provision for deliberately making the field non-uniform (field shaping).
5. The field must be established within the vacuum chamber of the pulser without affecting the system pressure.
6. The portions of the magnet located within the vacuum chamber must be easily removable to permit servicing of components within the chamber.

In order to meet the design requirements, it was decided to build a DC iron core magnet that would use a relatively small amount of power to develop the 5000 gauss, large volume magnetic field. Due to the configuration of the pulser, the diode shank could be used as one element of the iron core. However, in order to connect the diode shank to the rest of the magnetic circuit, it was necessary to use radial vacuum gap coupling through the vacuum chamber wall of the diode shank housing. Limited space within the vacuum chamber and the necessity of avoiding outgassing within the chamber dictated the placement of the field coil outside the chamber.

The general design of the pulser electromagnet is that of a conventional C-magnet of relatively large proportions. The magnet coil is located outside the back of the vacuum chamber and the iron core of the magnet enters the bottom of the vacuum chamber directly by way of a vacuum sealed flange. As mentioned

earlier, the magnetic field enters the upper part of the chamber by coupling magnetically to the internal iron diode shank across a radial gap. The iron core within the vacuum chamber is furnished with removable pole pieces that are adjacent to the 2-inch long working magnet gap. The plain parallel surface pole pieces can be replaced by shaped surface pole pieces to obtain non-uniform magnetic fields. Since only the central 4-inch diameter portion of the field will be effective in collimating the pulsed electrons, the uniformity of this part of the field should be constant within approximately 2 percent.

The magnetic circuit is designed by calculating the number of ampere turns required to furnish the maximum flux density of 5000 gauss. The basic magnetic circuit equation is:

$$B = \frac{4\pi NI}{l} \quad (1)$$

where  $B$  is the flux density in gauss,  $N$  is the number of turns on the coil,  $I$  is the coil current in amperes and  $l$  is the total "effective" length of all air (vacuum) gaps in centimeters.

The size of the magnet core is determined partly by the required size of the working field gap, and partly by the flux density required in the gap. The flux density in the iron core must be kept below the saturation flux density. An iron core with a cross-section of at least 28 square inches satisfies the above requirements.

It was decided that a strip or tape wound magnetic coil would provide the maximum number of ampere turns in the smallest space. The tape wound coil uses a series of circular, water cooled plates between the "pancake elements" of this coil to keep the coil temperature to a reasonable level. Each "pancake element" contains 104 turns of 2" x .015" copper tape wound with a 6-inch I.D. and an O.D. of about 10.4 inches. Since there are 8 pancake elements in series, the total number of turns is 832. The resistance of this coil at 50°C is on the order of 0.5 ohm so that a standard 40 volt 50 ampere-power supply can be used to pass up to 50 amperes through this coil for a total of about 40,000 ampere turns.

Cooling calculations indicate that we need a water flow of about 0.25 to 0.50 gallons per minute to keep the outlet water temperature in the range of 10°C to 20°C above the inlet water temperature.

### 3.2.2 Power Supply and Charging Network for PEBA Energy Store

In any pulsed electron beam annealing (PEBA) system, the power supply and charging network have the job of reenergizing the dielectric transmission line energy store after each PEBA pulse. Because charging occurs over a time scale on the order of seconds, the transmission line array can be treated as a single dc capacitance which is to be recharged after each pulse. In intermediate duty applications involving single sample tests or beam development experiments, where charging time is not of prime importance, the energy store may be easily charged using a Van de Graaff electrostatic generator. Although the charging process is slow, requiring, for example, as much as several minutes for the Spi-Pulse 5000 developmental processor, Van de Graaff generators are relatively inexpensive when compared to commercial high voltage power supplies. At the same time, they are virtually impervious to electrical transients caused by the PEBA pulse, and can thus be conveniently located in the same pressure vessel as the energy store, with little electrical isolation, and without expensive interconnecting high voltage cables.

More demanding PEBA applications, involving rapid repetitive pulsing, generally require higher charging currents that extend beyond the capabilities of Van de Graaff generators. Hence, the energy store must be charged using a large conventional transformer-type rectified power supply, which is often housed in an external oil tank, and connected to the energy store via a high voltage cable. At voltages above about 250 kV, the selection of a reliable cable becomes a difficult task. In addition, the electronic components of the power supply must be protected from the electrical transients of the fast PEBA discharge. Despite the engineering problems associated with power supply charging systems, however, they can be made to work reliably if properly designed. Of the numerous schemes for charging the energy store, most fall into one of two categories: those which charge through a resistive element, and those which charge by way of an intermediate energy storage element.

### 3.2.2.1 Resistive Charging

The simplest way to charge the energy storage capacitor is through a single series resistor, as depicted in Figure 4.

The power supply voltage  $V_s$  is preset to the desired charging voltage, and the energy store capacitance is allowed to slowly charge up through the resistor  $R$  via RC charging. The capacitor is discharged through the PEBA diode each time the trigger switch is closed, within a time duration that is negligibly small compared to the charging cycle. Charging of the store voltage  $V_c$  through  $R$  is thereafter governed by the exponential relation

$$V_c = V_s (1 - e^{-t/RC}) \quad (2)$$

If charging is allowed to continue for at least five RC time constants before the diode is pulsed again, then  $V_c$  will reach 99% of  $V_s$ , and be within accuracy levels acceptable for PEBA work. In practice, the RC time constant must be long enough so that the trigger switch can regain its dielectric integrity before the energy store is fully recharged. (Usually  $RC > 0.2$  sec.) The supply voltage  $V_s$  may also be stabilized to power line

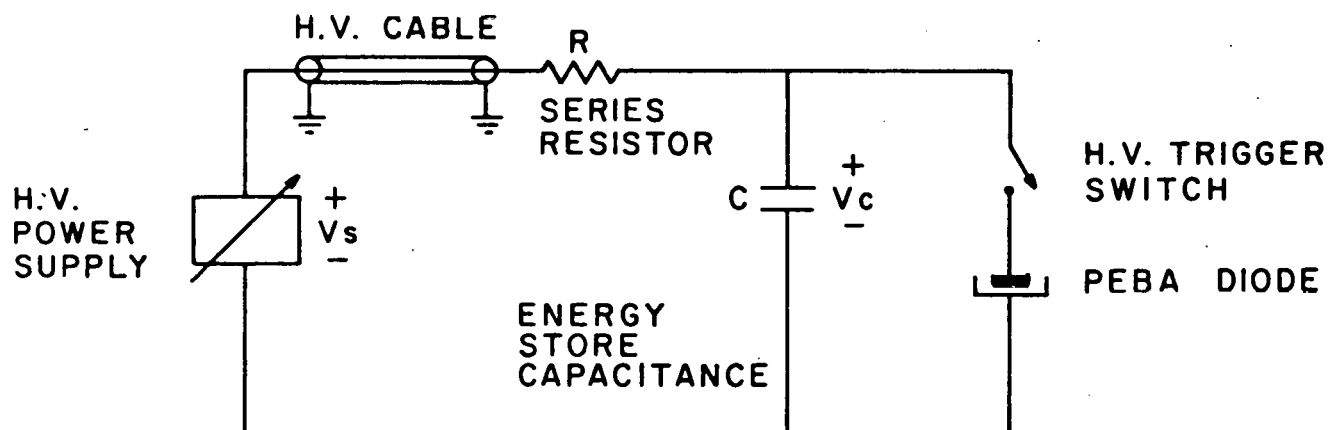


FIGURE 4. RESISTIVE CHARGING SCHEMATIC

variations by electromechanical regulation, if precise repeatability is required.

The selection of resistor R requires some consideration. The value of R must be orders of magnitude larger than the impedance of both the PEBA diode and transmission line store, so that it will not affect the transmission line discharge process. It must also be large enough to safely limit the surge current which flows from the power supply at the beginning of each charging cycle, but small enough so that the total recharge time is sufficiently short.

The chief disadvantage of the RC charging scheme is the energy lost to resistive heating. For a given amount of energy stored in the capacitor, an equal amount of energy must be dissipated in the resistor during the entire charging cycle, regardless of the value of R. This property can be derived by integrating the instantaneous power dissipated in the resistor over the entire exponential charging cycle:

$$P = \frac{(V_s - V_c)^2}{R} = \frac{V_s^2}{R} e^{-2t/RC} \quad (3)$$

$$\therefore E_{\text{dissipated}} = \int_{t=0}^{\infty} P dt = \frac{V_s^2}{R} \int_0^{\infty} e^{-2t/RC} = 1/2 C V_s^2 \quad (4)$$

which equals the stored capacitor energy, and is independent of R.

### 3.2.2.2 RC Charging System for 160 kV

In large capacity, high voltage PEBA systems, the amount of energy thus dissipated in the resistor can be substantial, requiring both a physically large charging resistor, and a scheme for removing the excess heat. However, the dissipated energy is proportional to the square of the charging voltage, and can thus become manageable at somewhat lower charging voltages. The specifications for an RC charging design, incorporating a specific 160 kV power supply now owned by Spire, are listed in Table 1. The system is adequate for the first phase tests of the PEBA section of the junction processor system.

TABLE 1. SPECIFICATIONS FOR RESISTIVE  
CHARGING WITH 160 kV SUPPLY

---

Power Supply Type	Universal Voltronics BAL-160-5.5E
Maximum Voltage	180 kV (no load)
Maximum Current	5.5 mA (at 160 kV)
Series Resistance (R)	35 M
Resistor Length	70 cm
Internal Resistance of Power Supply	1.8 M

	Minimum 7 Dielectric Lines	Maximum 19 Dielectric Lines
Energy Store Capacitance	20 nF	55 nF
Minimum Charge Time (SRC)	3.7 sec	10 sec
Total Dissipated Energy	325 joules	880 joules
Average Dissipated Power*	90 watts	90 watts
Estimated Temperature Rise at Surface of Charging Resistor	16°C	16°C
Estimated Temperature Rise at Surface of High Voltage Electrode	6°C	6°C

\*Averaged over entire charging cycle

---

The charging resistor in the system is physically oriented in the reentrant configuration inside one line of the multielement energy store, as illustrated in Figure 5. The other dielectric lines in the array are simultaneously charged through the common electrical connection at the bottom ends of the lines.

The reentrant design, which has been used successfully in other Spire electron beam processors, adds series inductance between the resistor and capacitor which helps protect both the resistor and power supply from electrical discharge transients. At the same time, physical space is conserved. The high voltage cable, in this case a solid polyethylene type with semiconducting shields, is protected against damaging ac voltage components by being electrically located on the supply side of the charging resistor, and thus always held at constant dc power supply voltage.

A simplified thermal analysis of resistor heating, based on the equations of coaxial heat flow, indicate a worst case steady state temperature rise of  $16^{\circ}\text{C}$  above ambient at the surface of the resistor. For room temperature ambient, the resistor temperature will thus be well below the  $170^{\circ}\text{C}$  heat distortion temperature of the thermal dielectric epoxy compound used to pot the resistor. A similar analysis of the heating of the dielectric line housing the resistor structure indicates a temperature rise of about  $6^{\circ}\text{C}$  at the inner electrode surface. Although the steady state temperature will thus also be below the  $49^{\circ}\text{C}$  heat distortion temperature of the high voltage dielectric used to make the line, the safety margin is much smaller. Heating should not be a problem, however, if the design of the lines and support structure allows the gas inside the pressure vessel to convect away some of the excess heat to the pressure vessel walls.

The dielectric polarization loss in the epoxy itself, caused by successive charge/discharge cycles, is of minor significance compared to the resistive heat loss experienced during charging.

### 3.2.2.3 Intermediate Storage Charging

When higher charging voltages are employed in the electron pulser, the heat loss inherent to the resistive charging method can become large, making other charging methods preferable. Several alternatives involve charging the energy store via an intermediate storage element, which temporarily processes all or part of the total stored energy. One such scheme, shown schematically in Figure 6,

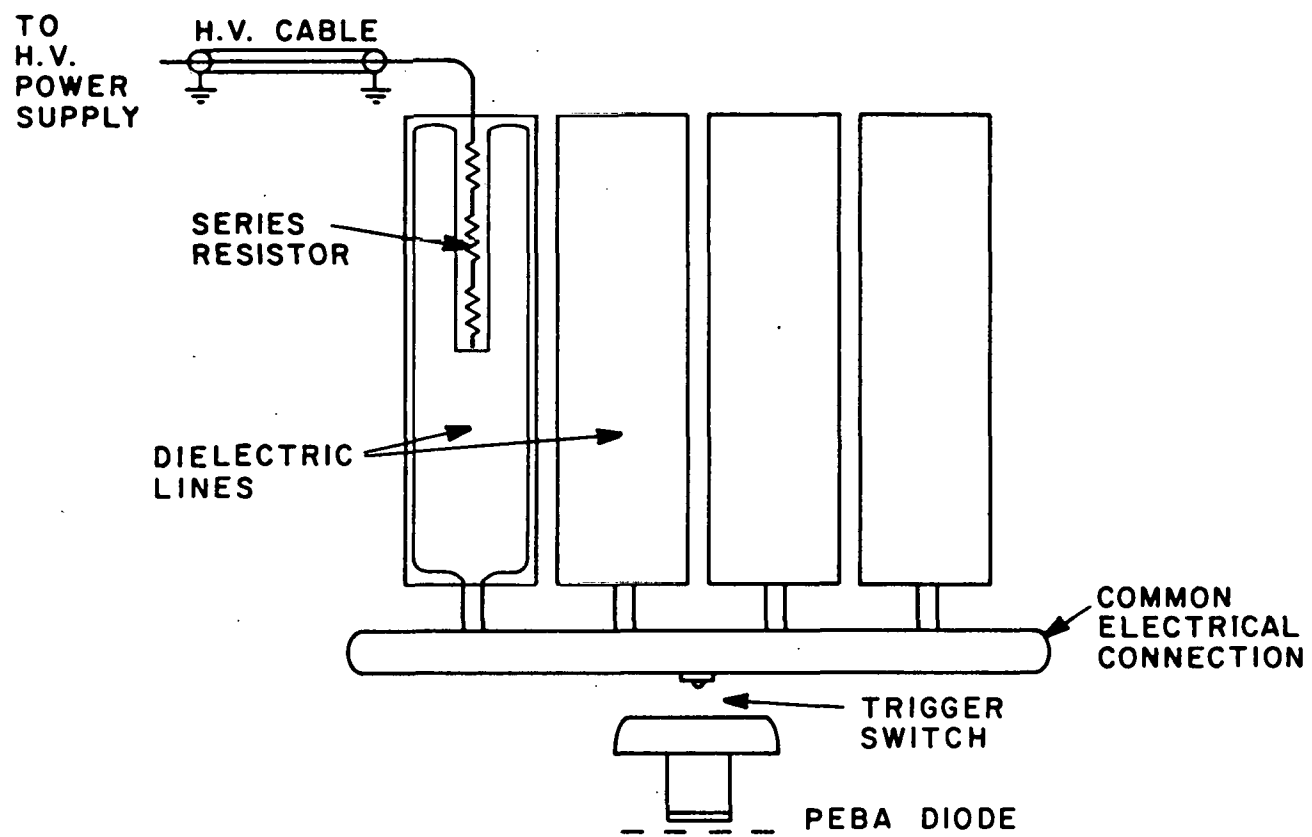


FIGURE 5. SERIES RESISTOR INCORPORATED INTO MULTI-ELEMENT DIELECTRIC LINE ENERGY STORE

incorporates the PEBA energy store capacitor in a voltage doubler circuit with additional components inside the power supply tank. The energy store capacitor  $C_2$  is charged sinusoidally by the combination of the transformer voltage  $V_t$  and capacitor voltage  $V_1$  in series. Operation of the circuit is easily understood if it is remembered that the voltage across the intermediate storage capacitor  $C_1$  is "refreshed", through diode  $D_1$ , to the peak transformer voltage  $-V_T$  each positive half cycle of  $V_t = V_T \sin \omega t$ . As  $V_t$  falls into its negative cycle, diode  $D_2$  closes at the point where:

$$V_T + V_1 = -V_2$$

or

$$V_t = -V_2 + V_T \quad (5)$$

since  $V_1 = -V_T$  just prior to the closing of  $D_2$ . Equation (5) defines the cut in voltage of  $V_t$  at which  $D_2$  closes as:

$$V_{\text{cut in}} = -V_2 + V_T \quad (6)$$

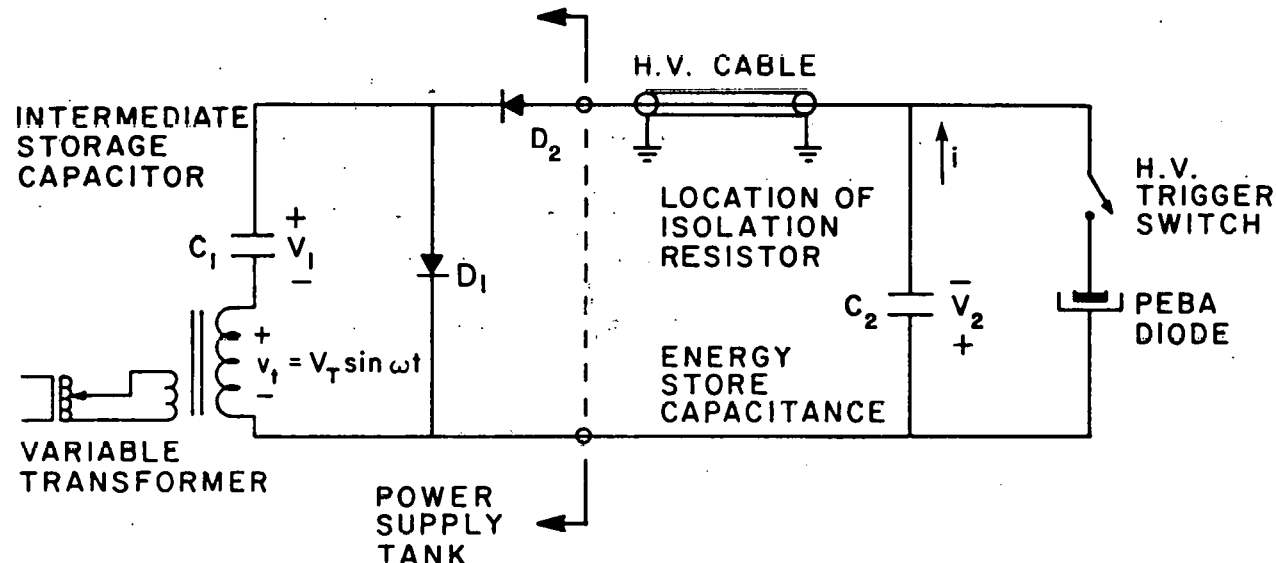


FIGURE 6. DIAGRAM OF INTERMEDIATE STORAGE ELEMENT CHARGING SYSTEM

As  $V_t$  continues to fall below the cut in voltage, it will execute a total voltage drop of

$$V_{\text{cut in}} - (-V_T) = 2V_T - V_2 \quad (7)$$

before reaching the negative peak. (During this phase,  $D_1$  is off, and  $D_2$  on), charge transfer from  $C_1$  to the energy store  $C_2$  will be governed by conservation of charge

$$dq_2 = dq_1 \quad (8)$$

and by the charge-voltage relationship for each capacitor

$$q_1 = C_1 V_1 \quad (9)$$

$$q_2 = C_2 V_2$$

The change in the series voltages  $\Delta(V_1 + V_2)$  must also be equal to the total change in  $V_t$  executed between the cut in point (1) and the negative peak of the cycle, i.e.

$$\Delta(V_1 + V_2) = V_{\text{cut in}} - (-V_T)$$

and substituting Equation (7) gives

$$\Delta(V_1 + V_2) = 2V_T - V_2 \quad (10)$$

From equations (8) - (10), the change in energy store voltage  $V_2$  over each sinusoidal cycle of the transformer can be derived:

$$\Delta V_2 = \frac{C_1}{C_1 + C_2} (2V_T - V_2) \quad (11)$$

Equation (11) describes the change in energy store voltage  $\Delta V_2$  experienced after each cycle of  $V_t$ , in terms of the voltage existing on the store before the cycle. By dividing Equation (11) by the period  $\Delta t = T$  of the transformer voltage cycle, an expression is created for the time rate of change of  $V_2$ :

$$\frac{\Delta V_2}{\Delta t} = \frac{C_1}{C_1 + C_2} \left( \frac{2V_T - V_2}{T} \right) \quad (12)$$

If the period  $T$  is much shorter than the overall charging time, (i.e., if  $\Delta V_2 \ll V_T$ ), then Equation (12) has the quasi-continuous exponential solution.

$$V_2 = 2 V_T \left[ 1 - \exp \left( \frac{-C_1}{C_1 + C_2} \frac{t}{T} \right) \right] \quad (13)$$

Hence, the charging of the energy store  $C_2$  is exponential in form, and will reach within .99 of the voltage  $2V_T$  after about five time constants  $5 \left( \frac{C_1 + C_2}{C_1} \right) T$ .

The charging current, when averaged over all the sinusoidal cycles of  $V_T$ , will likewise follow the exponential envelope

$$i = I_o \exp \left[ \frac{-C_1}{C_1 + C_2} \frac{t}{T} \right] \quad (14)$$

where

$$I_o = \frac{C_1 C_2}{C_1 + C_2} \frac{2V_T}{T}$$

It can be shown that the heat loss associated with the charging of both  $C_1$  and  $C_2$  become arbitrarily small as the circuit resistance approaches zero. Although the charging envelope is exponential, the transfer of charge over a given cycle occurs sinusoidally, and hence approaches the constant entropy (no loss) condition. The addition of an isolation resistor between the energy store and high voltage cable does produce an energy loss, but its magnitude can be minimized by choosing a small value for  $R$ . In practice, a value of  $10 \text{ K}\Omega$  to  $100 \text{ K}\Omega$  will insure adequate transient protection of the power supply components from the electron beam pulse.

### 3.2.2.4 Intermediate Storage Element Charging System for 300kV

In long-term production applications, the PEBA section of the junction processor may require voltages as high as 300 kV. The specifications for a charging system using the intermediate storage capacitor method are given in Table 2. The physical layout of energy store components is similar to that of Figure 5 for the 160 kV system.

TABLE 2. SPECIFICATIONS FOR INTERMEDIATE  
STORAGE CAPACITOR CHARGING AT 300 kV

Power Supply Type	Custom Design	
Peak Transformer Voltage $V_T$	150 - 170 kV	
Intermediate Storage Capacitance $C_i$	4 nF	
Series Isolation Resistance	10 K $\Omega$	
	Minimum	Maximum
	7 Dielectric Lines	19 Dielectric Lines
Energy Store Capacitance $C_z$	20 nF	55 nF
Peak Envelope Current $I_o$	60 mA	67 mA
Average Charging Current*	6 mA	17 mA
Minimum Charging Time	0.5 sec	1.3 sec
Average Power Dissipated in Resistor	.36 watts	3 watts
Estimated Temperature Rise at Surface of Isolation Resistor	negligible	0.5°C

\*Averaged over many sinusoidal cycles of transformer voltage.

### 3.2.2.5 RC Charging System for 300kV

Although the intermediate storage capacitor method is efficient and fast, and a good design choice for 300 kV charging levels, the commercial custom manufactured power supply components and tank may tend to be quite expensive. Listed in Table 3 are the specifications for a resistor charging scheme for use with a standard "off the shelf" 300 kV power supply. The implementation of resistive charging at 300 kV with the same repetition rate capability as the system specified in Table 3 will require the design of a forced cooling system utilizing air or freon gas. A cooling coil either wound around the outside of the resistor housing, or wound around the resistor body and imbedded in the thermal dielectric potting epoxy should be sufficient. The specifications for such a cooling system will be calculated if cost restrictions indicate RC charging as a design alternative at 300 kV.

TABLE 3. SPECIFICATIONS FOR RESISTIVE  
CHARGING USING 300 kV SUPPLY

---

<b>Power Supply Type</b>	<b>To be identified</b>	
<b>Maximum Voltage</b>	<b>300 kV</b>	
<b>Maximum Current</b>	<b>40 mA</b>	
<b>Series Resistance (R)</b>	<b>7.3 MΩ</b>	
<b>Resistor Length</b>	<b>70 cm</b>	
	<b>Minimum</b>	<b>Maximum</b>
	<b>7 Dielectric Lines</b>	<b>19 Dielectric Lines</b>
<b>Energy Store Capacitance</b>	<b>20 nF</b>	<b>55 nF</b>
<b>Minimum Charge Time (SRC)</b>	<b>0.75 sec</b>	<b>2 sec</b>
<b>Total Dissipated Energy</b>	<b>900 joules</b>	<b>2475 joules</b>
<b>Average Dissipated Power*</b>	<b>1240 watts</b>	<b>1240 watts</b>
<b>Estimated Temperature Rise at Surface of Charging Resistor Without Forced Cooling</b>	<b>220°C</b>	<b>220°C</b>
<b>Estimated Temperature Rise at Surface of High Voltage Electrode Without Forced Cooling</b>	<b>83°C</b>	<b>83°C</b>

---

\*Averaged over entire charging cycle.

### 3.2.3 Pressure Vessel and Energy Store Support Structure

The pressure vessel and internal support plates are designed to house a nested set of 19 parallel-charged coaxial transmission lines 9.5 inches in diameter by 4.4 feet long. The lines will be placed vertically in a hexagonal arrangement with the high-voltage input at the reentrant high-voltage termination charging the full array of lines through a common electrical connection (see Figure 5).

The capacitor support base plate will be a 438-pound, 65.5-inch diameter, 3/4-inch-thick steel perforated plate that will carry the full 1197-pound capacitor load with minimal deflection. A flame-sprayed aluminum coating 6-8 mils thick will be applied to retard corrosion and establish a good electrical ground path.

The upper 100-pound aluminum support plate, which will stabilize and center the array of capacitors, will be connected to the lower base plate with long steel tie rods.

The pressure vessel is being fabricated by Buffalo Tank Company, a division of Bethlehem Steel Corporation, and is scheduled for delivery at the end of August 1980. The 4000-pound vessel is designed with 5/16-inch-thick SA 285C steel walls to withstand the pressure of an insulating gas at 100 PSIG to suppress high-voltage flashover. The overall tank size is nominally 5 feet in diameter by 7 feet high with symmetrical domed end bells. The upper and lower end caps are sealed to the main tank body with an EMI/RFI shield gasketing manufactured by Metex Corporation that combines silicone rubber with a knitted metal mesh.

As supportive information for the design effort, a computer simulation program called FFEARS was used to solve Laplace's equation to compute an electrical model for the electric fields around the critical high-voltage stress regions within the high-voltage pulse-forming network. Of particular concern were the geometry and location of the edges of the common charge collection plate and the terminations of the capacitors. From plots of the computer data it was concluded that the electric fields around the collection plate would be below the breakdown strength of the surrounding dielectric gas. The electric field plots for the surface of the capacitor termination gave field values that were below one-half the breakdown threshold of the 1264 epoxy (400 volts/mil).

### 3.2.4 Interim Wafer-Handling System

An interim wafer-handling system is currently being designed and fabricated which will allow a single wafer to pass from a vacuum lock into the diode region of the process chamber and then out through an exit lock. The design and fabrication to Spire's specifications is being undertaken by Brooks Associates, Inc., North Billerica, Massachusetts, with the delivery of the complete system due by the end of September 1980. Each 6-inch entrance and exit lock has been designed to accommodate a wafer platen, if required, with dimensions of 5 inches square by 0.150 inch thick. A lock consists of two pass-through port valves, vestibule, transfer track and drive, pump port and vent valves, position sensor and porch track section.

The detailed design drawings for the wafer lifter mechanism have been completed, and the design requirements integrated into the diode/magnet gap transfer mechanism layout. The geometrical interference problems associated with the wafer movement in this narrow gap have been resolved by a relocation of the track drives.

### 3.2.5 Electronic Control

Functional and logic control diagrams are being formulated as part of the electronic design package for the overall system control. A representative functional block diagram for the SPI-PULSE 7000 is given in Figure 7.

The interrelationship of the major electronic subsystem control components is given in the SPI-PULSE 7000 system schematic presented in Figure 8.

### 3.2.6 Vacuum System

The vacuum process chamber where the pulsed electron beam annealing occurs is being fabricated from 1 1/2-inch-thick aluminum-plate stock for the top and bottom and 1-inch-thick plate stock for the sides. The chamber, weighing about 150 pounds, will be 40 inches long, 22 inches wide and 15 inches high. The completed chamber, after vacuum leak testing, is scheduled for delivery to Spire on 23 July 1980.

For oil-free high-vacuum pumping a CTI Cryo-Torr 8 high-performance cryopump has been ordered and received along with a 6-inch VRC air-operated gate valve. The roughing mechanical pump is a 14.1-CFM Leybold Heraeus Model D16A.

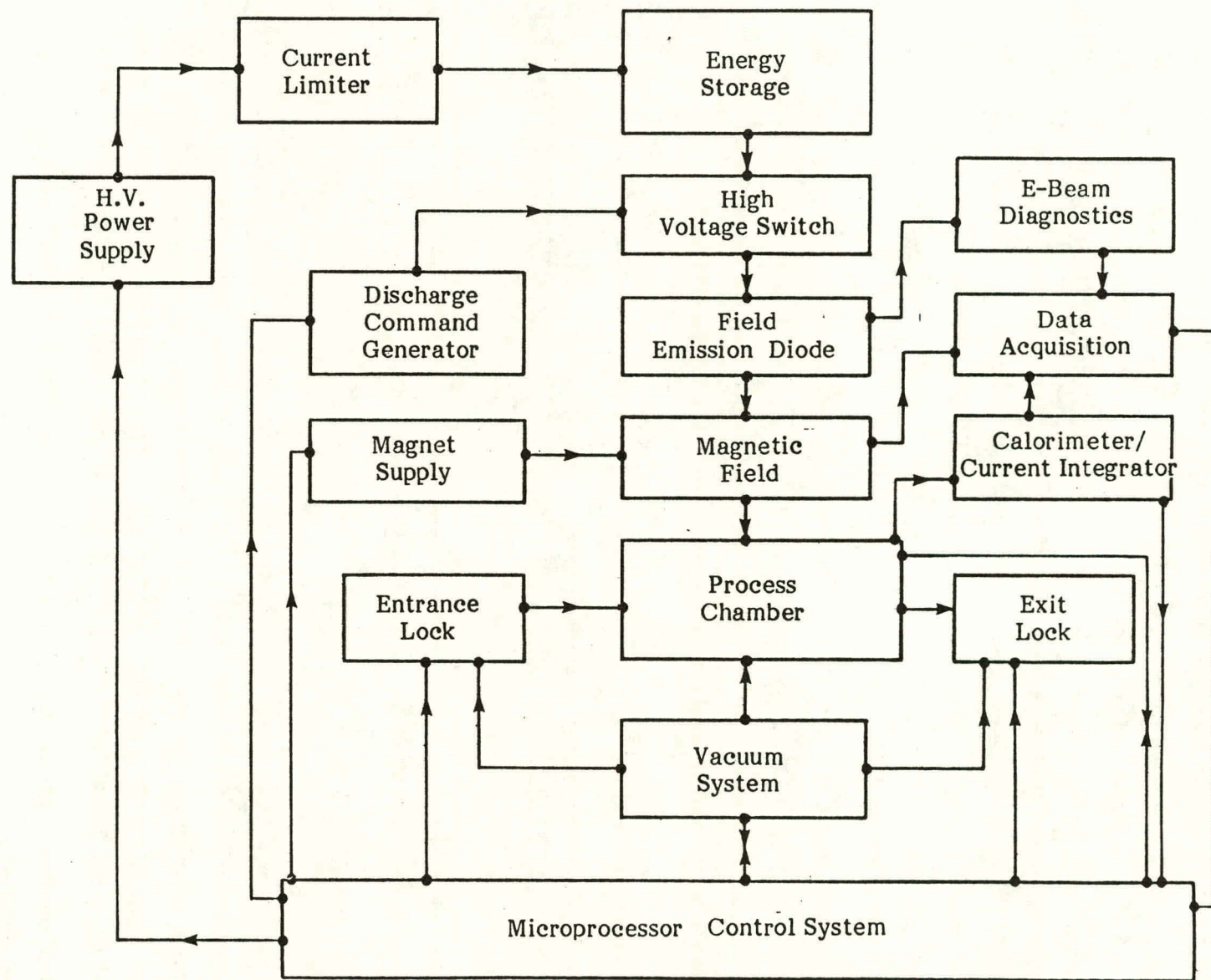


FIGURE 7. SPI-PULSE 7000 FUNCTIONAL BLOCK DIAGRAM

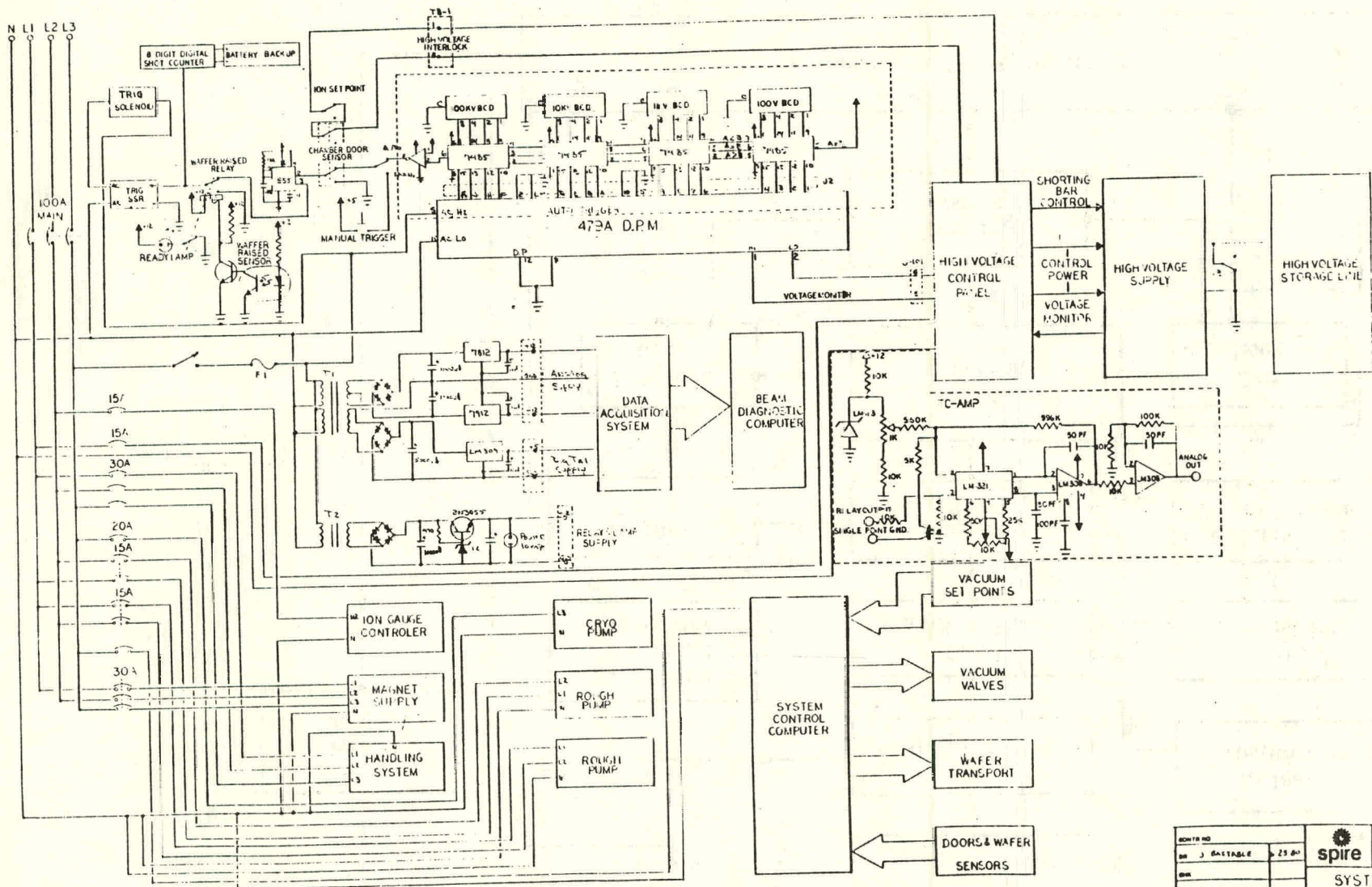


FIGURE 8. SPI-PULSE 7000 SYSTEM SCHEMATIC

SOHTR NO	SPIRE	SPIRE CORPORATION
SOH J 5151816	2501	BEDFORD MASS 01730
SHR	SYSTEM SCHEMATIC	
APP	SPI PULSE 7000	
APPD SOHTR DISCHARGE APPL	BJS CODE IDENT NO	SOHTR NO
SOHTR ACT APPL	D 4D656	214 9001
WEAK	SHEET 1 OF 1	

With this pumping system, process chamber contamination is eliminated as well as the need for additional cooling water and liquid nitrogen. Process chamber pressures, expected to be in the  $10^{-6}$ -torr range, will be monitored with a Granville-Phillips Model 270004 automatic-ranging ionization-gauge controller.

## SECTION 4

### PLANS

During the next reporting period additional storage lines will be molded, metallized and electrically tested for capacitance and insulation properties. Electrical console layout, interface support electronics and power distribution will continue as part of the electrical design effort.

With the major fabricated items such as the pressure vessel, magnet components and vacuum chamber arriving on schedule, assembly and hardware integration should be well underway by mid-September.

SECTION 5  
SCHEDULE

Figure 9 shows the projected schedule for Task 1, "Pulsed Electron Beam Subsystem Development".

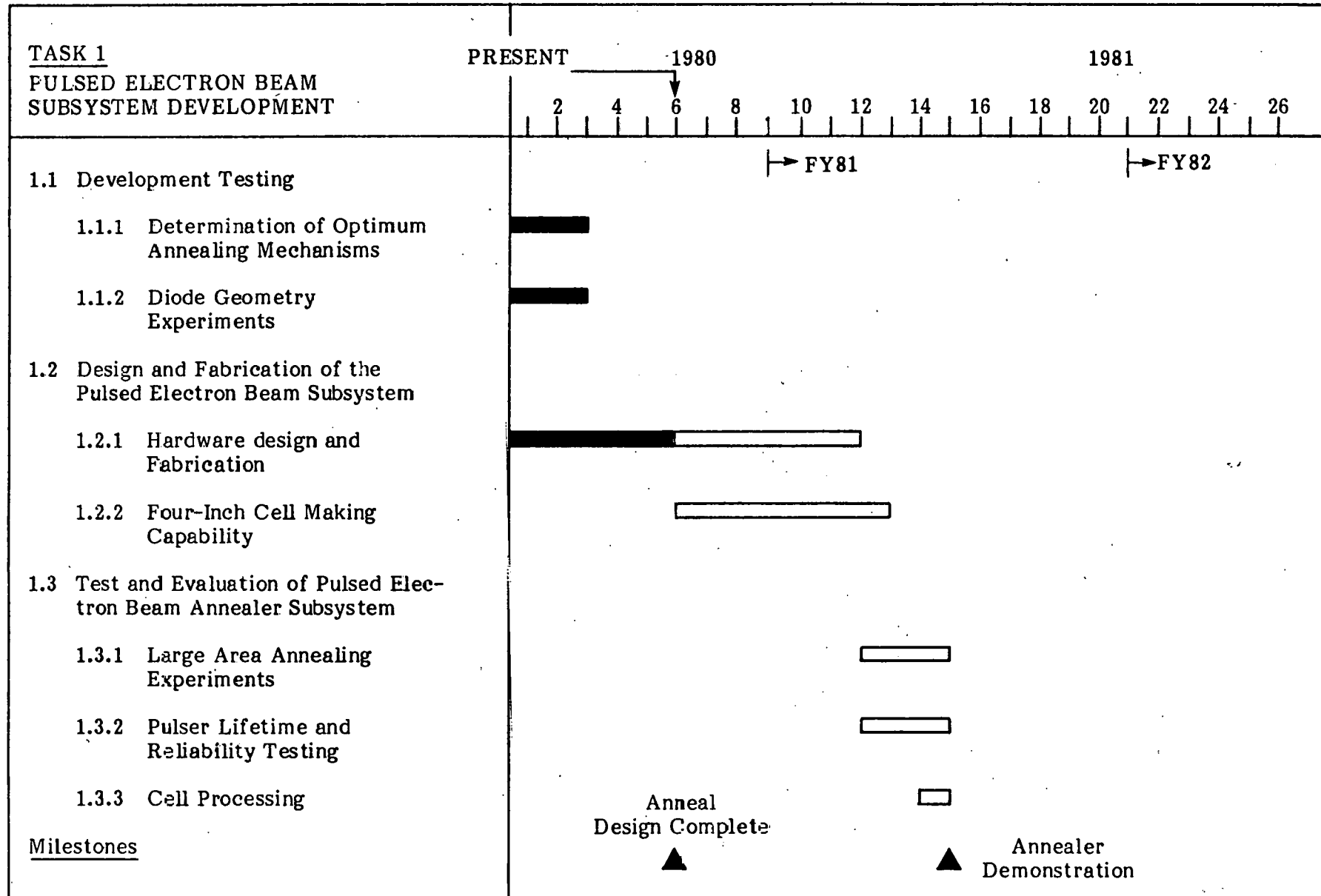


FIGURE 9. TASK 1 SCHEDULE